

Optimal Bounded Inversion for Nonminimum Phase Nonhyperbolic Systems

Linqi Ye, Yaqi Wang, Deshan Meng*, Xueqian Wang, Bin Liang

Abstract— Accurate tracking control of nonminimum phase systems relies on the calculation of the ideal internal dynamics (IID). Traditional IID calculation methods fail when applied to nonminimum phase nonhyperbolic systems (systems with nonhyperbolic zero dynamics). Recently, we propose the optimal bounded inversion method for IID calculation, which obtains IID by solving a trajectory optimization problem. In this paper, we extend our previous result and show that optimal bounded inversion can also deal with nonminimum phase nonhyperbolic systems. More than that, it is also possible to achieve different control goals by setting different cost functions. Particularly, three cases are investigated in this paper. The first uses minimal initial value deviation as the cost function, resulting in “T-IID” which can achieve accurate output tracking. The second applies minimal terminal value as the cost function, resulting in “S-IID” which leads to a final rest for the system. The last combines “T-IID” and “S-IID” to achieve a compound goal. The effectiveness is verified through Matlab simulations of a two-cart inverted-pendulum system.

I. INTRODUCTION

A system is nonminimum phase if it has unstable zeros (linear system) or unstable zero dynamics (nonlinear system) [1]. Output tracking of nonminimum phase systems is a challenging problem since traditional inversion-based methods will lead to unbounded input. To solve this problem, the concept of ideal internal dynamics (IID) was proposed in [2], which is a bounded solution of the internal states driven by the output reference. IID can be directly transformed into the reference state and feedforward input, which can be used to achieve accurate tracking for nonminimum phase systems.

To date, several methods have been developed to calculate the IID, which can be divided into three categories. One is the output regulation method [3,4], which obtains the reference trajectory for the state and input by solving a regulation equation. The second IID calculation method is stable system center [5,6], which builds an estimator to get the IID. However, in both methods, the output reference is assumed to be generated by a known exosystem, which restricts their applications to more general output references. Another method called stable inversion [7,8] builds a more general

Resrach supported by National Natural Science Foundation of China (No.62003188, No.61803221, and U1813216), and the Basic Research Program of Shenzhen (Grant JCYJ20180306174321766).

L. Ye, Y. Wang, X. Wang, and B. Liang are with the Center of Intelligent Control and Telescience, Tsinghua Shenzhen International Graduate School, Tsinghua University, 518055 Shenzhen, China (e-mail: ye.linqi@sz.tsinghua.edu.cn; yq-wang19@mails.tsinghua.edu.cn; wang.xq@sz.tsinghua.edu.cn; bliang@tsinghua.edu.cn).

D. Meng is with the School of Aeronautics and Astronautics, Sun Yat-Sen University, Shenzhen 518107, China, and also with the Shenzhen International Graduate School, Tsinghua University, Shenzhen 518055, China (e-mail: mengdsh3@mail.sysu.edu.cn)

framework to calculate IID, which can be applied to arbitrary output references. The key idea is based on a simple observation: backward integration of a purely unstable system converges to a bounded solution. Therefore, by decomposing the stable/unstable part of the zero dynamics, a Picard-like iteration can be applied to find a bounded solution [7,8]. Following [7,8], there have been a continued interest in improving the computation efficiency of the stable inversion method [9~12] and extending this method to discrete systems [13]. One problem of stable inversion is its noncausality: it requires to know all the future information of the output reference. To alleviate this, a preview-based method [14,15] was proposed, which only requires to know the output reference in a finite future time horizon.

However, the existing IID calculation methods have some limitations when applied to nonminimum phase nonhyperbolic systems. First, stable system center and stable inversion methods both fail in this case. By modifying the internal dynamics [16], approximate stable inversion can be achieved, where the resulted IID is approximate to the original system. Second, although some methods like output regulation [17] and a spline-based method [18] can solve accurate IID for linear systems, they can only get approximate solutions for nonlinear systems. Therefore, the accurate calculation of IID for nonminimum phase nonhyperbolic systems, especially nonlinear systems, still remains an open problem.

To sum up, IID calculation is difficult for nonlinear nonminimum phase systems, and is much more challenging for nonlinear nonminimum phase nonhyperbolic systems. It is of great significance to develop an algorithm that is easy to implement, high-precision, and widely applicable to all kinds of nonminimum phase systems. Recently, we propose the optimal bounded inversion method [20] for IID calculation, which transforms IID calculation into a trajectory optimization problem and solves it through the powerful MATLAB software GPOPS-II. In this paper, we explore to apply this method to nonminimum phase nonhyperbolic systems. To achieve different control goals, two well-designed optimization cost functions are proposed. One is to minimize the initial value deviation of the internal states, which results in “T-IID” that is able to achieve accurate tracking as much as possible. The other is to minimize the final value of the internal states, which leads to “S-IID” that reduces the final motion of the internal states as much as possible. These two options can be used independently or can be combined to realize different goals. The effectiveness is verified through Matlab simulations of a two-cart inverted-pendulum system.

The main contribution of this paper is the extension of the optimal bounded inversion method to nonminimum phase nonhyperbolic systems with multiple control goals. Through this paper and our previous paper [20], it verifies that optimal

bounded inversion is capable of IID calculation to different kinds of nonminimum phase systems. Meanwhile, optimal bounded inversion gives us some flexibility in IID calculation to achieve different control goals. Besides, it takes advantage of the GPOPS-II software, which guarantees high accuracy and is also very easy to implement. These features make it outperform other methods.

The rest of this paper is organized as follows. Section II introduces the concept of IID. Section III shows how to use optimal bounded inversion for IID calculation. Section IV presents the results of numerical simulations and Section V concludes this paper.

II. THE CONCEPT OF IID

Consider a nonlinear nonminimum phase system, denote $\mathbf{u} = [u_1, u_2, \dots, u_m]^T$ as the input vector, $\mathbf{y} = [y_1, y_2, \dots, y_m]^T$ as the output vector with the relative degree $\{r_1, r_2, \dots, r_m\}$, and $\boldsymbol{\eta}$ as the internal state vector. The system dynamics are given as follows:

$$\mathbf{y}^{(r)} = \mathbf{F}_1(\mathbf{x}) + \mathbf{G}_1(\mathbf{x})\mathbf{u} \quad (\text{External Dynamics}), \quad (1)$$

$$\dot{\boldsymbol{\eta}} = \mathbf{F}_2(\mathbf{x}) + \mathbf{G}_2(\mathbf{x})\mathbf{u} \quad (\text{Internal Dynamics}), \quad (2)$$

where $\mathbf{y}^{(r)} = [y_1^{(r_1)}, y_2^{(r_2)}, \dots, y_m^{(r_m)}]^T$ represent the high-order derivatives of the output (the order depends on when the input appears). $\mathbf{x} = [\boldsymbol{\xi}, \boldsymbol{\eta}]^T$ is the state vector, in which $\boldsymbol{\xi} = [y_1, \dot{y}_1, \dots, y_1^{(r_1-1)}, \dots, y_m, \dot{y}_m, \dots, y_m^{(r_m-1)}]^T$ represents the external state vector. Define $\mathbf{y}_r(t) = [y_{1r}(t), y_{2r}(t), \dots, y_{mr}(t)]^T$ as the output reference. Then the output tracking problem is to let \mathbf{y} track \mathbf{y}_r . Define \mathbf{x}_r as the state reference and \mathbf{u}_r as the input reference, which satisfy

$$\begin{aligned} \mathbf{y}_r^{(r)} &= \mathbf{F}_1(\mathbf{x}_r) + \mathbf{G}_1(\mathbf{x}_r)\mathbf{u}_r, \\ \dot{\boldsymbol{\eta}}_r &= \mathbf{F}_2(\mathbf{x}_r) + \mathbf{G}_2(\mathbf{x}_r)\mathbf{u}_r, \end{aligned} \quad (3)$$

where $\mathbf{x}_r = [\boldsymbol{\xi}_r, \boldsymbol{\eta}_r]^T$ with $\boldsymbol{\xi}_r$ being the external state reference and $\boldsymbol{\eta}_r$ being the internal state reference. Then we can achieve accurate output tracking by using the following linear tracking controller:

$$\mathbf{u} = \mathbf{u}_r + \mathbf{K}(\mathbf{x} - \mathbf{x}_r), \quad (4)$$

where \mathbf{u}_r is the feedforward input and $\mathbf{K}(\mathbf{x} - \mathbf{x}_r)$ is a feedback of state error with \mathbf{K} is a gain matrix. Actually, (4) is widely used in output regulation [3] as well as stable inversion [7,8]. It can be interpreted as: the feedforward \mathbf{u}_r provides the needed control input for precision output tracking, while the feedback $\mathbf{K}(\mathbf{x} - \mathbf{x}_r)$ generates a correction input when the system states deviate from the state reference and thus keeps the system stable.

The external state reference trajectory can be directly derived by $\boldsymbol{\xi}_r = [y_{1r}, \dot{y}_{1r}, \dots, y_{1r}^{(r_1-1)}, \dots, y_{mr}, \dot{y}_{mr}, \dots, y_{mr}^{(r_m-1)}]^T$.

However, the internal state reference trajectory $\boldsymbol{\eta}_r$ is not easy to attain.

Solving \mathbf{u}_r from the first equation in (3) gives

$$\mathbf{u}_r = \mathbf{G}_1(\mathbf{x}_r)^{-1} [\mathbf{y}_r^{(r)} - \mathbf{F}_1(\mathbf{x}_r)]. \quad (5)$$

Substituting (5) into (3) gives:

$$\dot{\boldsymbol{\eta}}_r = \mathbf{F}_2(\mathbf{x}_r) + \mathbf{G}_2(\mathbf{x}_r)\mathbf{G}_1(\mathbf{x}_r)^{-1} [\mathbf{y}_r^{(r)} - \mathbf{F}_1(\mathbf{x}_r)]. \quad (6)$$

which are the zero dynamics corresponding to the regulated output $\mathbf{e} = \mathbf{y} - \mathbf{y}_r$.

For simplicity, denote the right hand side in (6) as $\boldsymbol{\varphi}(\boldsymbol{\eta}_r, \boldsymbol{\xi}_r)$, then the zero dynamics driven by the output reference can be written as

$$\dot{\boldsymbol{\eta}}_r = \boldsymbol{\varphi}(\boldsymbol{\eta}_r, \boldsymbol{\xi}_r). \quad (7)$$

Since the system is nonminimum phase, the zero dynamics (7) is unstable, which means direct integration of the zero dynamics will give an unbounded solution. To achieve accurate output tracking and guarantee stability of the internal dynamics at the same time, we need to find a bounded solution (that is, the IID) for the unstable zero dynamics and then stabilize the internal states to the IID. Therefore, IID builds a bridge between output tracking and internal dynamics stabilization as shown in Fig. 1.

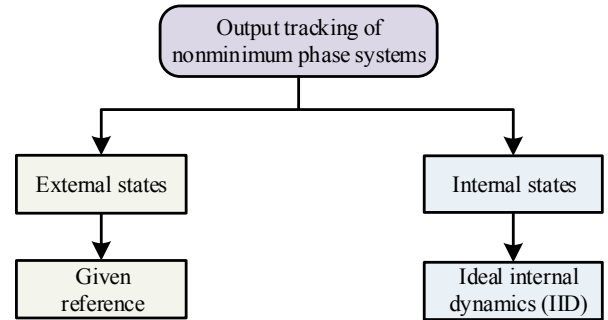


Figure 1. Relationship between output tracking and internal dynamics stabilization.

Once the IID $\boldsymbol{\eta}_r$ is obtained, then $\mathbf{x}_r = [\boldsymbol{\xi}_r, \boldsymbol{\eta}_r]^T$ is known and \mathbf{u}_r can be obtained from (5) so that $\mathbf{x}_r, \mathbf{u}_r$ can be applied to the tracking controller (4) to achieve accurate output tracking. To sum up, the output tracking problem of a nonminimum phase system can be reduced to finding a bounded solution (that is, the IID $\boldsymbol{\eta}_r$) for the zero dynamics (7) which is driven by the output reference.

In the literature, IID usually means a bounded solution in infinite time interval, that is, $t \in (-\infty, +\infty)$. However, in the real situation, a tracking control task is always executed in finite time. Correspondingly, we can define finite-time IID as the internal state trajectory within a given boundary $\boldsymbol{\eta}_{\min} \leq \boldsymbol{\eta} \leq \boldsymbol{\eta}_{\max}$ for a finite time interval $t \in [t_0, t_f]$.

For illustration, consider the following nonminimum phase system

$$\begin{aligned} \dot{\xi} &= u, \\ \dot{\eta} &= \eta + \xi, \\ y &= \xi. \end{aligned} \quad (8)$$

Assume the reference trajectory is $y_r = \sin t$. Then the internal dynamics driven by the output reference is

$$\dot{\eta} = \eta + \sin t. \quad (9)$$

Fig. 2 shows a bunch of solutions which satisfy (9). It can be seen that most of the solutions diverge quickly and will go to infinity as $t \rightarrow \infty$. However, there is a bounded solution

$$\eta = -\frac{1}{2} \cos t - \frac{1}{2} \sin t \text{ for } t \in [0, +\infty), \text{ which is the IID.}$$

What's more, if we limit the time interval in $t \in [0, 20]$ and the state boundary to $\eta \in [-5, 5]$, then we can find numerous solutions within this region, which are the finite-time IID. In the later sections, we will focus on the calculation of the finite-time IID, and if not specifically stated, we refer to "finite-time IID" when we say "IID".

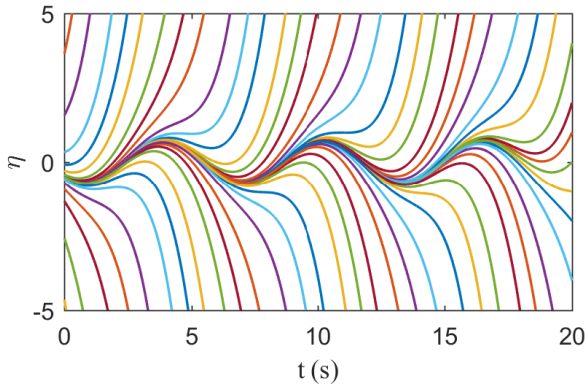


Figure 2. Solutions for (9).

III. THE OPTIMAL BOUNDED INVERSION METHOD

As shown in the previous section, IID is a bounded solution concerning time for the internal states when the outputs move along the given reference trajectories. In other words, IID is a bounded solution for the differential equation of the internal dynamics when the outputs are constrained in the reference trajectories, which is depicted in Fig. 3.

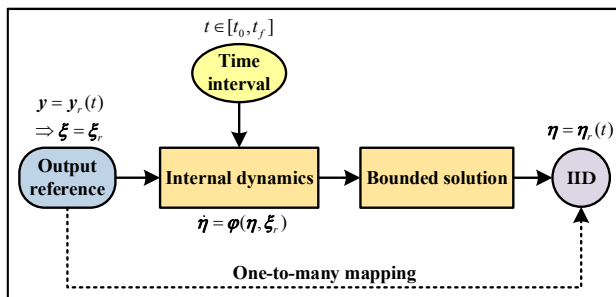


Figure 3. The IID calculation problem.

If we only consider state boundary in IID calculation, it is a one-to-many mapping from the output reference to IID. Still use (9) for illustration, Fig. 4 shows the $y_r \rightarrow \eta_r$ mapping for

two output references. It can be seen that an output reference leads to a group of IID.

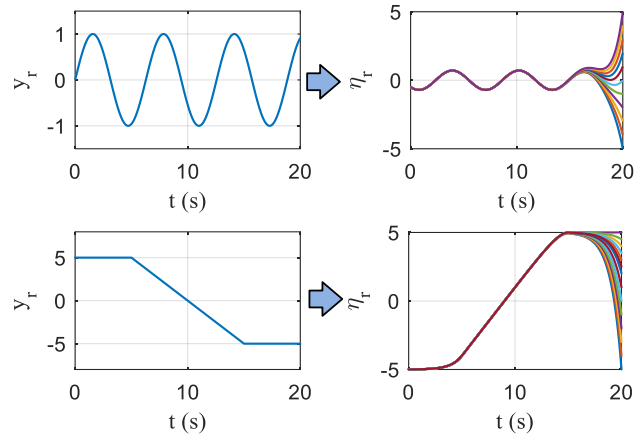


Figure 4. One-to-many mapping from output reference to IID.

In order to restrict the output reference-IID relationship to a one-to-one mapping, an additional condition is required. In the stable inversion method [7, 8], a boundary condition is inserted which transforms IID calculation into a bounded value problem. The idea is shown in Fig. 5. It divides the zero dynamics into two parts, including an unstable part η_u and a stable part η_s . Then the initial value for η_s and the terminal value for η_u are selected as specified bounded values ($\eta_s(t_0)$ can be obtained from the initial state values while $\eta_u(t_f)$ is usually set to zero).

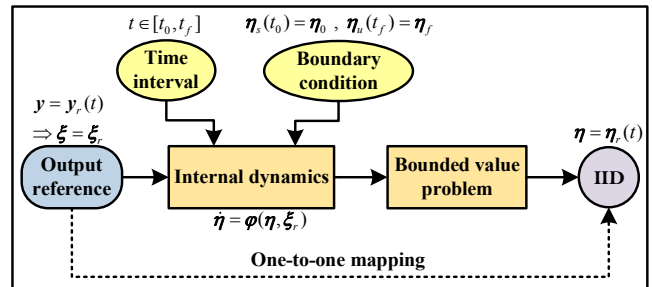


Figure 5. IID calculation by stable inversion.

When using stable inversion to (9), it leads to the one-to-one IID as shown in Fig. 6.

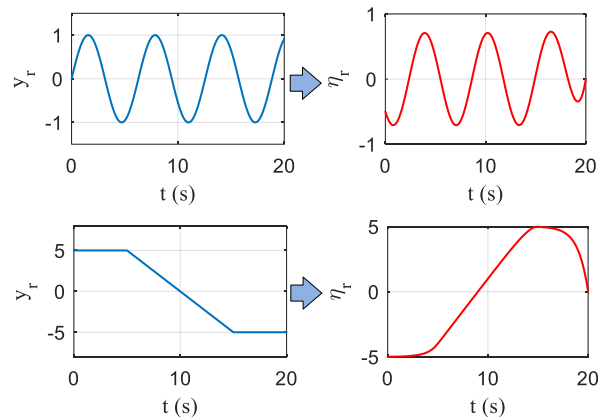


Figure 6. One-to-one mapping from output reference to IID by stable inversion.

For nonminimum phase nonhyperbolic systems, the linearized zero dynamics are nonhyperbolic, meaning the existence of eigenvalues with zero real part. In this case, the zero dynamics cannot be simply divided into stable/unstable part, which disables the use of stable inversion method. However, the optimal bounded inversion method we proposed in [20] can be applied in this case. Unlike stable inversion, optimal bounded inversion does not require system decomposition. Instead, it calculates IID through trajectory optimization.

The idea of optimal bounded inversion is shown in Fig. 7, where state constraints are added to keep the internal states in the desired boundary, and a cost function is designed to achieve specific control goals as well as to ensure the one-to-one mapping property.

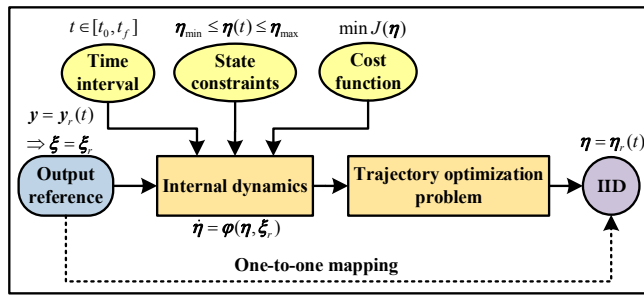


Figure 7. IID calculation by optimal bounded inversion.

Optimal bounded inversion gives us some flexibility in designing the cost function. Different cost functions will result in different IID. For (9), when using minimal terminal absolute value as the cost function, it leads to the same results as obtained by stable inversion. If we select minimal terminal absolute change rate as the cost function, it leads to a different IID as shown in Fig. 8.

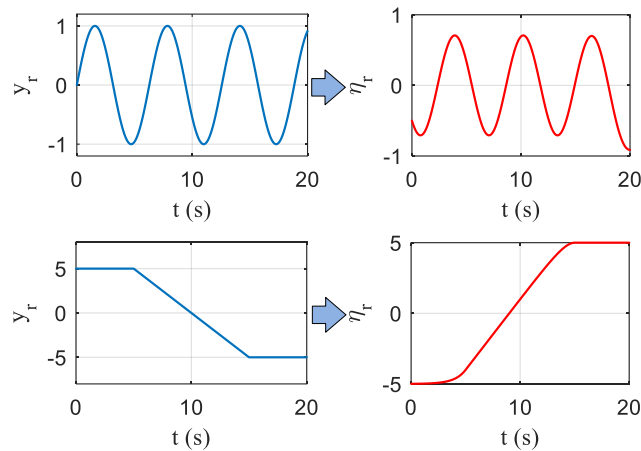


Figure 8. One-to-one mapping from output reference to IID by optimal bounded inversion.

Following is a formal description of the optimal bounded inversion method. Consider the zero dynamics (7), suppose the desired boundary for the internal state is $\eta_r \in [\eta_{\min}, \eta_{\max}]$. We construct the following trajectory optimization problem to calculate the IID.

Optimal bounded inversion problem: Giving an output reference trajectory y_r in $t \in [t_0, t_f]$ (t_0 is the start time and t_f is the end time, and y_r can be transformed into the external state reference ξ_r), determine a trajectory $\eta_r(t)$ which satisfies: 1) the zero dynamics constraint $\dot{\eta}_r = \varphi(\eta_r, \xi_r)$; 2) the state constraint $\eta_{\min} \leq \eta_r \leq \eta_{\max}$; and 3) minimizes a cost function J .

The cost function determines the final solution of the IID, which is important to the control performance. Here we give two candidates for the cost function.

(1) Minimal initial value deviation

$$J = \|\eta(t_0) - \eta_r(t_0)\|. \quad (10)$$

This cost function represents the initial value deviation between the internal states and the IID. Minimizing it can reduce the initial tracking error and thus improve the tracking accuracy. For convenience, we call the resulted IID ‘‘T-IID’’, where the letter ‘‘T’’ represents tracking.

(2) Minimal final motion

$$J = \|\dot{\eta}_r(t_f)\| = \|\varphi(\eta_r(t_f), t_f)\| \quad (11)$$

This cost function represents the magnitude of the final change rate for the internal states. Minimizing it can suppress the motion of the internal states in the end as much as possible. The resulted IID is very suitable when the system is expected to stop tracking and come to a final rest. Therefore, we call it ‘‘S-IID’’, where ‘‘S’’ means stopping.

The optimal bounded inversion problem defined above is a standard trajectory optimization problem, which can be conveniently solved by using the software GPOPS-II [19]. The resulted T-IID and S-IID can be used for different purposes and can also be combined to achieve a compound goal. For example, T-IID can be used at the beginning of a tracking task to ensure accurate tracking while S-IID can be used when the tracking task is finished, and the system is expected to come to a final rest.

IV. NUMERICAL SIMULATIONS

In this section, the optimal bounded inversion method is applied to a two-cart inverted-pendulum system [16,17], which is a benchmark system with nonhyperbolic zero dynamics. The system is shown in Fig. 9.

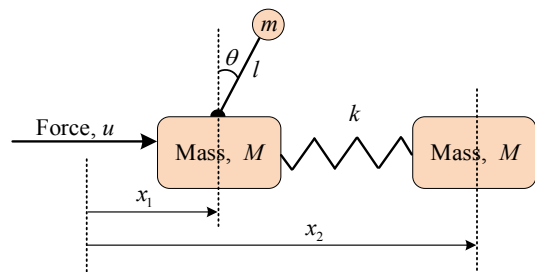


Figure 9. Two-cart inverted-pendulum system.

Following [17], the dynamic equations of the system are written as follow:

$$\begin{aligned}
\dot{x}_1 &= v_1, \\
\dot{v}_1 &= \frac{1}{M + m \sin^2 \theta} \left[u + ml\omega^2 \sin \theta - bv_1 \right. \\
&\quad \left. - mg \cos \theta \sin \theta + k(x_2 - x_1) \right], \\
\dot{x}_2 &= v_2, \\
\dot{v}_2 &= \frac{k}{M} (x_1 - x_2), \\
\dot{\theta} &= \omega, \\
\dot{\omega} &= \frac{1}{(M + m \sin^2 \theta)l} \left[(M + m)g \sin \theta - u \cos \theta \right. \\
&\quad \left. + bv_1 \cos \theta - ml\omega^2 \sin \theta \cos \theta - k(x_2 - x_1) \cos \theta \right], \\
y &= x_1,
\end{aligned} \tag{12}$$

where x_1 is the position and v_1 is the velocity of the left cart, x_2 is the position and v_2 is the velocity of the right cart. θ, ω are the pendulum angle and angular rate. The parameters are: M is the mass of the cart, l is the length of the pendulum, m is the mass of the ball on the pendulum, g is the gravitational acceleration, k is the spring constant, and b is the viscous friction coefficient. In this system, the applied force u is the input, and we select the position of the left cart x_1 as the output.

From (5), the input reference is obtained as

$$\begin{aligned}
u_r &= \left[M + m \sin^2 \theta_r \right] \dot{v}_{1r} - ml\omega_r^2 \sin \theta_r \\
&\quad + bv_{1r} + mg \cos \theta_r \sin \theta_r - k(x_{2r} - x_{1r}).
\end{aligned} \tag{13}$$

and the zero dynamics are

$$\begin{aligned}
\dot{x}_{2r} &= v_{2r}, \\
\dot{v}_{2r} &= \frac{k}{M} (x_{1r} - x_{2r}), \\
\dot{\theta}_r &= \omega_r, \\
\dot{\omega}_r &= \frac{1}{(M + m \sin^2 \theta_r)l} \left[(M + m)g \sin \theta_r - u_r \cos \theta_r \right. \\
&\quad \left. + bv_1 \cos \theta_r - ml\omega_r^2 \sin \theta_r \cos \theta_r - k(x_{2r} - x_{1r}) \cos \theta_r \right].
\end{aligned} \tag{14}$$

In the simulation, the model parameters are as follows: $M = 1.378 \text{ kg}$, $m = 0.051 \text{ kg}$, $l = 0.325 \text{ m}$, $g = 9.8 \text{ m/s}^2$, $k = 10 \text{ N/s}$, and $b = 12.98 \text{ kg/s}$. The tracking controller is given by (4) with $\mathbf{K} = [4.82, 15.9, -4.41, -1.71, 35.9, 6.32]$ and $\mathbf{x} = [x_1, v_1, x_2, v_2, \theta, \omega]^T$. The output reference is given as follows:

$$y_r = \begin{cases} 0, & \text{if } t < 5 \\ 1 - e^{-0.0004(t-5)^5}, & \text{if } 5 \leq t < 13 \\ 1 - e^{-0.0004(21-t)^5}, & \text{if } 13 \leq t < 21 \\ 0, & \text{if } t \geq 21. \end{cases} \tag{15}$$

Then $x_{1r} = y_r, v_{1r} = \dot{y}_r, \dot{v}_{1r} = \ddot{y}_r$ can be obtained from (15). And the IID is obtained by using the optimal bounded inversion method. To guarantee boundedness, the boundaries of the internal states are all chosen as $[-2, 2]$. The initial state is $\mathbf{x}(0) = \mathbf{0}$ and the time interval is 0~30s.

To verify the proposed method, three cases are considered in the simulation. Case 1: Tracking control with T-IID; Case 2: Tracking control with S-IID; and Case 3: Tracking control with a compound IID.

For Case 1 and Case 2, the resulted T-IID and S-IID are depicted in Fig. 10. It can be seen that the initial values of the T-IID are both zero, which are the same as the real initial conditions, but x_{2r} has an oscillation in the end. As for S-IID, it can be seen that both states come to a full stop in the end but θ_r has a big initial mismatch. Fig. 11 shows the simulation results when using T-IID in the tracking controller. It can be observed that the output achieves accurate tracking throughout the process. However, the internal states oscillate in the end which is undesired. Fig. 12 shows the simulation results when using S-IID in the tracking controller. It can be seen that the output has a tracking error at the beginning due to the initial mismatch, but the internal states are finally stabilized to zero.

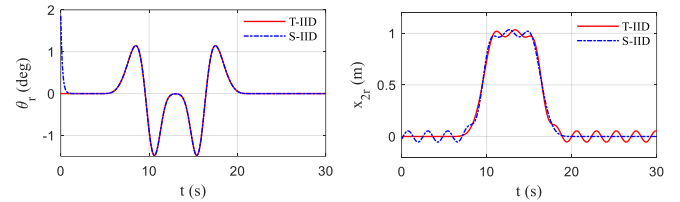


Figure 10. T-IID and S-IID.

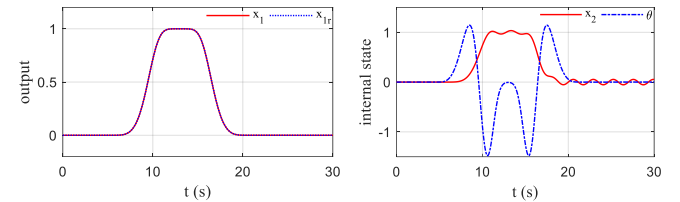


Figure 11. Simulation results with T-IID.

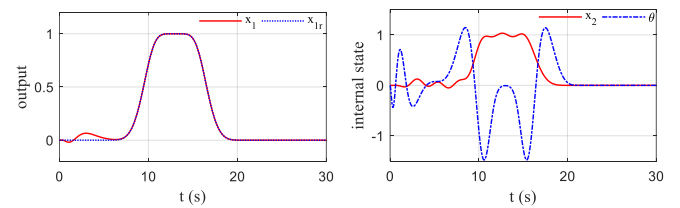


Figure 12. Simulation results with S-IID.

For case 3, it is assumed that the control task is divided into two parts by $t = 14\text{s}$, where precision tracking is expected in the first half and a final rest is expected in the second half. In this case, a compound IID can be used, where T-IID is applied to $t \in [0, 14]$ to guarantee precision tracking and S-IID is applied to $t \in [14, 30]$ to achieve a final rest. The simulation results are shown in Fig. 13 and Fig. 14. From Fig. 13, it can be seen that the output tracks very well with the

reference before $t = 14$ s and then has a small deviation, finally stopping at the desired value. From Fig. 14, it can be observed that the IID x_{2r}, θ_r have a small step change at $t = 14$ s which is due to the transition from T-IID to S-IID. This strategy guarantees that the internal states come to a final rest. To sum up, the compound IID can achieve accurate tracking at the desired time interval as well as stabilizes the internal states to a final rest status.

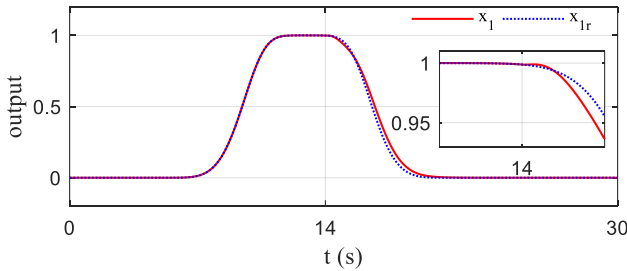


Figure 13. Output curve with compound IID.

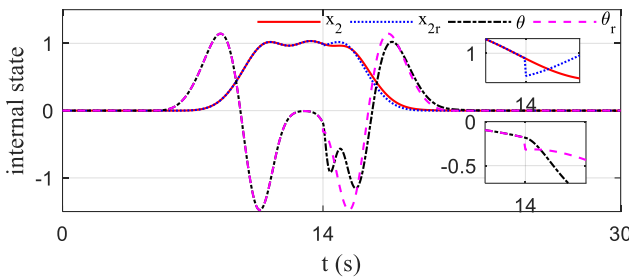


Figure 14. Internal state curve with compound IID.

V. CONCLUSION

Optimal bounded inversion is investigated in this paper to calculate the ideal internal dynamics (IID) for nonminimum phase nonhyperbolic systems and thus achieve precision output tracking. Optimal bounded inversion calculates IID from the perspective of trajectory optimization, making it possible to deal with nonhyperbolic zero dynamics. Two different optimization goals are defined which lead to two kinds of IID that can be used for different purposes. The two-cart inverted-pendulum example verify that the proposed method is suitable for systems with nonhyperbolic zero dynamics. Therefore, optimal bounded inversion gives a general solution for IID calculation and output tracking of different kinds of nonminimum phase systems, which is easy to implement, high-precision, and widely applicable.

REFERENCES

- [1] A. Isidori, *Nonlinear control systems*. Springer Science & Business Media, 2013.
- [2] S. Gopalswamy and H.J. Karl, "Tracking nonlinear non-minimum phase systems using sliding control," *Int. J. Control*, vol. 57, no. 5, pp. 1141-1158, 1993.
- [3] J. Huang, *Nonlinear output regulation: theory and applications*. SIAM, 2004.
- [4] C.I. Byrnes, F.D. Priscoli, and A. Isidori, *Output regulation of uncertain nonlinear systems*. Springer Science & Business Media, 2012.
- [5] I.A. Shkolnikov and Y.B. Shtessel, "Tracking controller design for a class of nonminimum-phase systems via the method of system center," *IEEE Trans. Autom. Control*, vol. 46, no. 10, pp. 1639-1643, 2001.

- [6] I.A. Shkolnikov and Y.B. Shtessel, "Tracking in a class of nonminimum-phase systems with nonlinear internal dynamics via sliding mode control using method of system center," *Automatica*, vol. 38, no. 5, pp. 837-842, 2002.
- [7] S. Devasia, D. Chen, and B. Paden, "Nonlinear inversion-based output tracking," *IEEE Trans. Autom. Control*, vol. 41, no. 7, pp. 930-942, 1996.
- [8] L.R. Hunt and G. Meyer, "Stable inversion for nonlinear systems," *Automatica*, vol. 33, no. 8, pp. 1549-1554, 1997.
- [9] D.G. Taylor and S. Li, "Stable inversion of continuous-time nonlinear systems by finite-difference methods," *IEEE Trans. Autom. Control*, vol. 47, no. 3, pp. 537-542, 2002.
- [10] T. Sogo, "On the equivalence between stable inversion for nonminimum phase systems and reciprocal transfer functions defined by the two-sided Laplace transform," *Automatica*, vol. 46, no. 1, pp. 122-126, 2010.
- [11] K. Graichen, V. Hagenmeyer, and M. Zeitz, "A new approach to inversion-based feedforward control design for nonlinear systems," *Automatica*, vol. 41, no. 12, pp. 2033-2041, 2005.
- [12] O. Bruls and R. Seifried, "A stable inversion method for feedforward control of constrained flexible multibody systems," *J. Comput. Nonlinear Dyn.*, vol. 9, no. 1, pp. 1-9, 2014.
- [13] W. Ohnishi, T. Beauduin, and H. Fujimoto, "Preactuated Multirate Feedforward Control for Independent Stable Inversion of Unstable Intrinsic and Discretization Zeros," *IEEE-ASME Trans. Mechatron.*, 2019, DOI: 10.1109/TMECH.2019.2896237.
- [14] Q. Zou and S. Devasia, "Precision preview-based stable-inversion for nonlinear nonminimum-phase systems: The VTOL example," *Automatica*, vol. 43, no. 1, pp. 117-127, 2007.
- [15] Q. Zou, "Optimal preview-based stable-inversion for output tracking of nonminimum-phase linear systems," *Automatica*, vol. 45, no.1, pp. 230-237, 2009.
- [16] S. Devasia, "Approximated stable inversion for nonlinear systems with nonhyperbolic internal dynamics," *IEEE Trans. Autom. Control*, vol. 44, no. 7, pp. 1419-1425, 1999.
- [17] J. Huang, "Asymptotic tracking of a nonminimum phase nonlinear system with nonhyperbolic zero dynamics," *IEEE Trans. Autom. Control*, vol. 45, no. 3, pp. 542-546, 2000.
- [18] L. Jetto, V. Orsini, and R. Romagnoli, "Accurate output tracking for nonminimum phase nonhyperbolic and near nonhyperbolic systems," *Eur. J. Control*, vol. 20, no. 6, pp. 292-300, 2014.
- [19] M.A. Patterson and A.V. Rao, "GPOPS-II: A MATLAB software for solving multiple-phase optimal control problems using hp-adaptive Gaussian quadrature collocation methods and sparse nonlinear programming," *ACM Trans. Math. Softw.*, vol. 41, no.1, pp. 1-37, 2014.
- [20] L. Ye, Q. Zong, and B. Tian, "Output Tracking of Uncertain Nonminimum Phase Systems by Experience Replay," *IEEE Transactions on Systems, Man, and Cybernetics: Systems*, DOI: 10.1109/TSMC.2019.2919012, 2019.